

Partially Bio-based Poly(amide imide)s by Polycondensation of Aromatic Diacylhydrazides Based on Lignin-Derived Phenolic Acids and Aromatic Dianhydrides: Synthesis, Characterization, and Computational Studies

Sachin S. Kuhire,^{1,2} Pragati Sharma,^{2,3} Suman Chakrabarty,³ Prakash P. Wadgaonkar ^{1,2}

¹Polymers and Advanced Materials Laboratory, Polymer Science and Engineering Division, CSIR-National Chemical Laboratory, Pune 411008, India

²Academy of Scientific and Innovative Research, New Delhi 110025, India

³Physical and Materials Chemistry Division, CSIR-National Chemical Laboratory, Pune 411008, India

Correspondence to: P. P. Wadgaonkar (E-mail: pp.wadgaonkar@ncl.res.in) or S. Chakrabarty (E-mail: s.chakrabarty@ncl.res.in)

Received 14 June 2017; accepted 28 July 2017; published online 00 Month 2017

DOI: 10.1002/pola.28748

ABSTRACT: Two new bio-based diacylhydrazide monomers, namely, 4,4'-(propane-1,3-diylbis(oxy))bis(3-methoxybenzohydrazide) and 4,4'-(propane-1,3-diylbis(oxy))bis(3,5-dimethoxybenzohydrazide) were synthesized starting from lignin-derived phenolic acids, namely, vanillic acid and syringic acid. A series of poly(amide imide)s was synthesized by polycondensation of these diacylhydrazide monomers with commercially available aromatic dianhydrides. Poly(amide imide)s showed inherent viscosity in the range 0.44–0.56 dL g^{−1} and exhibited good solubility in organic solvents. Poly(amide imide)s could be cast into transparent, flexible, and tough films from their *N,N*-dimethylacetamide solutions. Poly(amide imide)s showed 10% weight loss in the temperature range 340–364 °C indicating

their good thermal stability. Glass transition temperature (*T*_g) of poly(amide imide)s were measured by DSC and DMA which were in the range 201–223 °C and 214–248 °C, respectively. The *T*_g values of poly(amide imide)s were dependent on the number methoxy substituents on aromatic rings of diacylhydrazide monomers. Molecular dynamics simulation studies revealed that chain rigidity is the dominant factor for observed trends in *T*_g. © 2017 Wiley Periodicals, Inc. *J. Polym. Sci., Part A: Polym. Chem.* **2017**, 00, 000–000

KEYWORDS: computational studies; lignin; renewable resources; step-growth polymers; structure-property relations

INTRODUCTION In the recent years, bio-based polymers have attracted a great deal of attention due to the environmental issues and depletion of non-renewable resources.^{1–4} A large number of bio-based polymers are already being manufactured in industry.^{5,6} Most of the bio-based polymers are aliphatic or cyclo-aliphatic in nature and are derived from vegetable oils, cellulose, or starch.^{7,8} However, aliphatic and cyclo-aliphatic polymers have limited applications due to their poor mechanical properties, low thermal stability, and low glass transition temperatures (*T*_gs).^{9–11} On the other hand, polymers containing aromatic units exhibit higher thermal stability, higher *T*_g, and better mechanical properties.^{12,13} However, relatively a limited number of examples are available wherein aromatic polymers have been synthesized from bio-derived chemicals such as lignin,^{14–16} furan derivatives,¹⁷ pentadecylphenol,^{18,19} terpene,²⁰ eugenol,²¹ 4-aminophenylalanine,²² and so forth. Of these, lignin is the most abundant source of bio-based aromatic chemicals.²³ Around 70 million tonnes of lignin is produced annually as a

by-product of paper and pulp industries in the world. Depolymerization of lignin yields various phenolic derivatives such as vanillin, syringaldehyde, vanillic acid, syringic acid, syringol, guaiacol, ferulic acid, eugenol, and so forth.²⁴

The presence of functional groups in these aromatic chemicals offers interesting possibilities to use them as precursors for synthesis of useful monomers. Thus, a range bio-based monomers and polymers have been synthesized from lignin-derived aromatics,^{14,25} which include (meth)acrylic polymers,²⁶ epoxy polymers,²⁷ polybenzoxazines,²⁸ cyanate ester resins,²⁹ polycarbonates,³⁰ polyesters,^{31–34} poly(ether ester)s,^{14,35} polyacetals,³⁶ polyurethanes,^{37,38} and so forth.

Aromatic poly(amide imide)s represent an important class of high performance polymers due to their excellent thermal and mechanical properties.^{12,39–41} The excellent properties of poly(amide imide)s are derived from their distinctive chemical structure, which combine both amide and imide

Additional Supporting Information may be found in the online version of this article.

© 2017 Wiley Periodicals, Inc.

functional groups in the polymer backbone. Therefore, poly(amide imide)s find applications in several fields such as gas separation, nanofiltration, osmotic power generation, high temperature adhesives, electronic wire enamels, and so forth.^{42,43} A spectacular progress has been made in the field of poly(amide imide)s in terms of chemical structures, monomers, methods/techniques of synthesis, and the application areas.^{42,44–48}

With an objective to use lignin-derived phenolic acids as precursors for monomers useful for synthesis of high performance/temperature polymers, we wish to report herein the synthesis and characterization of new bio-based diacylhydrazide monomers, namely, 4,4'-(propane-1,3-diylbis(oxy))bis(3-methoxybenzohydrazide) (DVHzC-3) and 4,4'-(propane-1,3-diylbis(oxy))bis(3,5-dimethoxybenzohydrazide) (DSHzC-3). The key precursors used for the synthesis of monomers were vanillic acid, syringic acid, and 1,3-dibromopropane. A series of partially bio-based poly(amide imide)s was synthesized by polycondensation of diacylhydrazides with commercially available aromatic dianhydrides, namely, pyromellitic dianhydride (PMDA), 3,3',4,4'-biphenyltetracarboxylic dianhydride (BPDA), and 3,3',4,4'-oxydiphthalic anhydride (ODPA) via thermal cyclo-imidization process. Poly(amide imide)s were characterized by inherent viscosity measurements, solubility tests, FT-IR, ¹H NMR, and ¹³C NMR spectroscopy, elemental analysis, X-ray diffraction, thermogravimetric analysis (TGA), differential scanning calorimetric (DSC) studies, and dynamic mechanical analysis (DMA). The effect of number of methoxy substituents on aromatic rings on *T_g* of poly(amide imide)s was investigated. Furthermore, to understand the molecular origin of the substituent effects on *T_g*, molecular dynamics (MD) simulation studies were performed.

EXPERIMENTAL

Materials

Vanillic acid (97%), syringic acid (95%), and 1,3-dibromopropane (99%) were received from Sigma Aldrich, St. Louis, USA. Methyl vanillate and methyl syringate were prepared as reported in our previous article.³⁷ PMDA, BPDA, and ODPA were received from Sigma Aldrich, St. Louis, USA and sublimed under reduced pressure before use. Hydrazine hydrate (80%), ethanol, methanol, *N,N*-dimethylacetamide (DMAc), and other solvents were received from Thomas Baker Ltd. Mumbai, India, and were purified as per literature procedures.⁴⁹

Measurements

Melting points were recorded on Electrothermal MEL-TEMP apparatus and are uncorrected. FT-IR spectra were recorded on a Perkin-Elmer Spectrum GX spectrometer. ¹H and ¹³C NMR spectra were recorded on a Bruker-AV 200, 400, or 500 MHz spectrometer using dimethyl sulfoxide-*d*₆ or chloroform-*d* as solvent and TMS as an internal standard. HRMS was carried out on a Thermo Scientific Q-Exactive, Accela 1250 pump. Elemental analyses were performed with Flash EA 1112 elemental analyzer.

Inherent viscosity of poly(amide imide)s was measured with 0.5% (w/v) solution of polymer in DMAc using Ubbelohde suspended level viscometer at 30 ± 0.1 °C. Molecular weights and dispersity values of poly(amide imide)s were determined on Thermo-Finnigan make gel-permeation chromatography (GPC) using *N,N*-dimethylformamide (DMF) as an eluent at a flow rate of 1 mL min⁻¹ at 25 °C. Sample concentration was 2 mg mL⁻¹ and narrow dispersity polystyrenes were used as calibration standards. X-ray diffraction patterns of poly(amide imide)s were recorded using dried polymer film on a Rigaku Dmax 2500 X-ray diffractometer at a tilting rate of 2° min⁻¹. TGA was performed on Perkin Elmer: STA 6000 instrument at heating rate of 10 °C min⁻¹ under nitrogen atmosphere. *T_g* was determined on TA instruments DSC Q-10 with heating rate of 10 °C min⁻¹ under nitrogen atmosphere. *T_g* of polymer was recorded on second heating cycles. DMA of poly(amide imide)s as a function of temperature was determined on films cast from DMAc solutions. The sample dimensions were 10 × 6 mm (length × width) and thickness was in the range 0.09–0.13 mm. The measurements were carried out on Rheometrics Scientifics (Model Mark IV, UK), using the dynamic mode between 50 and 300 °C, at frequency of 1 Hz and heating rate of 5 °C min⁻¹.

Preparations

General Procedure for Synthesis of α , ω -Diester Containing Oxypropylene Linkage

Into a 250-mL two-necked round bottomed flask equipped with a reflux condenser and an argon inlet were charged, methyl vanillate or methyl syringate (40 mmol), potassium carbonate (22.1 g, 160 mmol) and *N,N*-dimethylformamide (100 mL). The reaction mixture was heated at 100 °C for 1 h and then 1, 3-dibromopropane (20 mmol) was added and heating was continued for 12 h. The reaction mixture was poured into ice cold water (250 mL). The precipitate was filtered and dissolved in dichloromethane (100 mL). The dichloromethane solution was washed with water (2 × 100 mL), dried over anhydrous sodium sulphate, filtered, and concentrated under reduced pressure. The crude product was purified by column chromatography using pet ether:ethyl acetate as an eluent to afford white solid. The product was recrystallized from ethanol:water mixture.

Dimethyl 4,4'-(propane-1,3-diylbis(oxy))bis(3-methoxybenzoate)

Yield: 80%; mp 158 °C; ¹H NMR (200 MHz, CDCl₃, δ /ppm): 2.35–2.48 (m, 2H), 3.90 (s, 12H), 4.30 (t, 2H), 6.94 (d, 2H), 7.54 (d, 2H), 7.64 (dd, 2H). ¹³C NMR (50 MHz, CDCl₃, δ /ppm): 28.9, 52.0, 56.0, 65.4, 111.7, 112.3, 122.8, 123.4, 148.9, 152.2, 166.8. Anal. calcd for C₂₁H₂₄O₈: C, 62.37; H, 5.98. Found: C, 62.18; H, 5.85.

Dimethyl 4,4'-(propane-1,3-diylbis(oxy))bis(3,5-dimethoxybenzoate)

Yield: 76%; mp 120 °C; ¹H NMR (200 MHz, CDCl₃, δ /ppm): 2.12–2.24 (m, 2H), 3.83 (s, 12H), 3.91 (s, 6H), 4.30 (t, 4H), 7.27 (s, 4H); ¹³C NMR (50 MHz, CDCl₃, δ /ppm): 31.0, 52.2,

56.1, 70.7, 106.7, 124.9, 141.5, 153.1, 166.8. Anal. calcd for $C_{23}H_{28}O_{10}$: C, 59.48; H, 6.08. Found: C, 58.97; H, 5.85.

General Procedure for Synthesis of α , ω -Diacylhydrazide Containing Oxypropylene Linkage

Into a 250-mL two necked round bottom flask equipped with a magnetic stirrer and a reflux condenser were placed α , ω -diester (28 mmol) and ethanol (50 mL). Hydrazine hydrate (80%; 28 g) was added dropwise to the reaction mixture over a period of 15 min and the reaction mixture was refluxed for 12 h. The solid that separated out was filtered, dried, and recrystallized from ethanol:water mixture.

4,4'-(Propane-1,3-diylbis(oxy))bis(3-methoxybenzohydrazide) (DVHzC-3)

Yield: 90%; mp 208 °C; 1H NMR (200 MHz, DMSO- d_6 , δ /ppm): 2.16–2.22 (m, 2H), 3.79 (s, 6H), 4.16 (t, 4H), 4.42 (s, 4H), 7.04 (d, 2H), 7.41 (d, 2H), 7.43 (dd, 2H), 9.63 (s, 2H); ^{13}C NMR (50 MHz, DMSO- d_6 , δ /ppm): 28.6, 55.6, 64.9, 110.5, 112.2, 120.1, 125.7, 148.4, 150.2, 165.6; HRMS (ESI, m/z): $[M + H]^+$ calcd for $C_{19}H_{25}N_4O_6$, 405.1769; found, 405.1768. Anal. calcd for $C_{19}H_{24}N_4O_6$: C, 56.43; H, 5.98; N, 13.85. Found: C, 56.41; H, 5.42; N, 13.97.

4,4'-(Propane-1,3-diylbis(oxy))bis(3,5-dimethoxybenzohydrazide) (DSHzC-3)

Yield: 97%; mp 222 °C; 1H NMR (200 MHz, DMSO- d_6 , δ /ppm): 1.87–2.0 (m, 2H), 3.76 (s, 12H), 4.09 (t, 4H), 4.47 (s, 4H), 7.15 (s, 4H), 9.71 (br. s, 2H); ^{13}C NMR (50 MHz, DMSO- d_6 , δ /ppm): 30.6, 55.9, 69.8, 104.4, 128.2, 138.9, 152.7, 165.4; HRMS (ESI, m/z): $[M + H]^+$ calcd for $C_{21}H_{29}N_4O_8$, 465.1980; found, 465.1975. Anal. calcd for $C_{21}H_{28}N_4O_8$: C, 54.30; H, 6.08; N, 12.06. Found: C, 54.24; H, 5.74; N, 12.36.

Synthesis of Poly(amide imide)s Containing Oxypropylene Linkages

General Procedure for Synthesis of Poly(amide imide)s from DVHzC-3/DSHzC-3 and Aromatic Dianhydrides

Into a 50-mL three-necked round bottom flask equipped with a guard tube, a nitrogen inlet, and a magnetic stirring bar were charged DVHzC-3/DSHzC-3 (1.20 mmol) and DMAc (10 mL). After complete dissolution of diacylhydrazide, aromatic dianhydride (1.20 mmol) was added in one portion to the stirred solution of diacylhydrazide. The reaction was allowed to proceed for an additional 12 h under nitrogen atmosphere. At the end of the reaction time, the viscous solution of poly(hydrazide acid) was obtained. The solution of poly(hydrazide acid) was cast onto a glass plate and the solvent was evaporated by heating at 80 °C with continuous nitrogen flow for 1 h. The semi-dried film was heated at 230 °C/0.75 mm Hg for 12 h under reduced pressure to effect imidization.

Synthesis of PAI-1 from DSHzC-3 and PMDA

FT-IR (cm^{-1}): 3237 (—NH stretching), 1795 (C=O asymmetrical), 1743 (C=O symmetrical), 1680 (C=O amide), 1338 (C—N—C stretching), 730 (C—N—C bending); 1H NMR (500 MHz, DMSO- d_6 , δ /ppm): 1.99–2.04 (m, 2H), 3.85 (s, 12H), 4.19 (t, 4H), 7.36 (s, 4H), 8.55 (s, 2H), 11.51 (s, 2H); ^{13}C

NMR (125 MHz, DMSO- d_6 , δ /ppm): 30.6, 56.1, 69.9, 105.4, 119.2, 125.2, 135.4, 140.4, 153.0, 163.8, 164.7. Anal. calcd for $C_{31}H_{26}N_4O_{12}$: C, 57.59; H, 4.05; N, 8.67. Found: C, 56.97; H, 4.65; N, 8.65.

Synthesis of PAI-2 from DSHzC-3 and BPDA

FT-IR (cm^{-1}): 3236 (—NH stretching), 1790 (C=O asymmetrical), 1742 (C=O symmetrical), 1680 (C=O amide), 1340 (C—N—C stretching), 723 (C—N—C bending); 1H NMR (400 MHz, DMSO- d_6 , δ /ppm): 2.0–2.07 (m, 2H), 3.85 (s, 12H), 4.19 (t, 4H), 7.35 (s, 4H), 8.16 (dd, 2H), 8.44 (d, 2H), 8.52 (d, 2H), 11.36 (s, 2H); ^{13}C NMR (100 MHz, DMSO- d_6 , δ /ppm): 30.4, 55.9, 69.7, 105.1, 122.9, 124.4, 125.3, 129.2, 130.4, 134.3, 140.1, 144.7, 152.8, 164.5, 164.9. Anal. calcd for $C_{37}H_{30}N_4O_{12}$: C, 61.50; H, 4.18; N, 7.75. Found: C, 61.10; H, 4.30; N, 7.56.

Synthesis of PAI-3 from DSHzC-3 and ODPA

FT-IR (cm^{-1}): 3240 (—NH stretching), 1789 (C=O asymmetrical), 1742 (C=O symmetric), 1680 (C=O amide), 1346 (C—N—C stretching), 722 (C—N—C bending); 1H NMR (200 MHz, DMSO- d_6 , δ /ppm): 1.92–2.05 (m, 2H), 3.83 (s, 12H), 4.17 (t, 4H), 7.32 (s, 4H), 7.73 (dd, 2H), 7.79 (d, 2H), 8.10 (d, 2H), 11.31 (s, 2H); ^{13}C NMR (50 MHz, DMSO- d_6 , δ /ppm): 30.6, 56.1, 69.9, 105.3, 114.7, 125.2, 125.4, 126.6, 132.4, 140.3, 153.0, 161.1, 164.7, 164.8. Anal. calcd for $C_{37}H_{30}N_4O_{13}$: C, 60.16; H, 4.09; N, 7.59. Found: C, 59.82; H, 3.84; N, 7.37.

Synthesis of PAI-4 from DVHzC-3 and PMDA

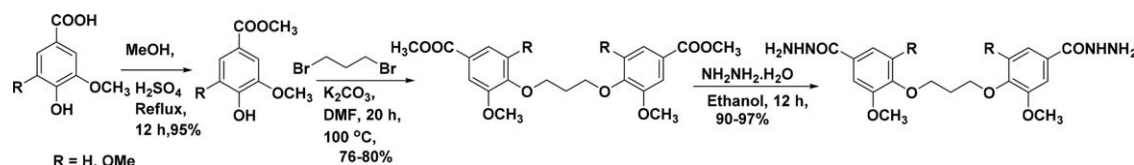
FT-IR (cm^{-1}): 3240 (—NH stretching), 1790 (C=O asymmetrical), 1741 (C=O symmetric), 1677 (C=O amide), 1339 (C—N—C stretching), 727 (C—N—C bending); 1H NMR (400 MHz, DMSO- d_6 , δ /ppm): 2.25–2.31 (m, 2H), 3.87 (s, 6H), 4.27 (t, 4H), 6.56 (d, 2H), 7.22 (d, 2H), 7.59 (s, 2H), 7.65 (d, 2H), 8.53 (s, 2H), 11.41 (s, 2H); ^{13}C NMR (100 MHz, DMSO- d_6 , δ /ppm): 28.5, 55.7, 65.1, 111.0, 112.3, 119.2, 121.7, 122.7, 135.4, 148.7, 151.8, 163.8, 163.9, 164.8. Anal. calcd for $C_{29}H_{22}N_4O_{10}$: C, 59.39; H, 3.78; N, 9.55. Found: C, 58.84; H, 4.14; N, 9.13.

Synthesis of PAI-5 from DVHzC-3 and BPDA

FT-IR (cm^{-1}): 3239 (—NH stretching), 1794 (C=O asymmetrical), 1741 (C=O symmetric), 1678 (C=O amide), 1345 (C—N—C stretching), 720 (C—N—C bending); 1H NMR (400 MHz, DMSO- d_6 , δ /ppm): 2.20–2.30 (m, 2H), 3.85 (s, 6H), 4.25 (t, 4H), 7.20 (d, 2H), 7.56 (s, 2H), 7.63 (d, 2H), 7.70 (d, 2H), 7.78 (s, 2H), 8.90 (d, 2H), 11.21 (s, 2H); ^{13}C NMR (100 MHz, DMSO- d_6 , δ /ppm): 28.5, 55.7, 65.1, 111.0, 112.3, 114.6, 121.6, 122.9, 125.1, 125.5, 126.6, 132.4, 148.7, 151.7, 161.1, 164.8, 164.9. Anal. calcd for $C_{35}H_{26}N_4O_{10}$: C, 63.44; H, 3.96; N, 8.46. Found: C, 62.52; H, 3.78; N, 8.46.

Synthesis of PAI-6 from DVHzC-3 and ODPA

FT-IR (cm^{-1}): 3237 (—NH stretching), 1794 (C=O asymmetrical), 1739 (C=O symmetric), 1678 (C=O amide), 1340 (C—N—C stretching), 734 (C—N—C bending); 1H NMR (400 MHz, DMSO- d_6 , δ /ppm): 2.27 (br. s, 2H), 3.85 (s, 6H), 4.25 (t, 4H), 7.19 (dd, 2H), 7.56 (dd, 2H), 7.60 (d, 2H), 7.66 (d, 2H),



SCHEME 1 Synthesis of diacylhydrazides starting from vanillic/syringic acid.

7.78 (d, 2H), 8.09 (d, 2H), 11.21 (s, 2H); ^{13}C NMR (100 MHz, $\text{DMSO}-d_6$, δ/ppm) 28.5, 55.7, 65.1, 111.0, 112.4, 114.7, 121.6, 122.8, 126.6, 132.4, 148.6, 151.7, 161.1, 164.8, 164.9. Anal. calcd for $\text{C}_{35}\text{H}_{26}\text{N}_4\text{O}_{11}$: C, 61.95; H, 3.86; N, 8.26. Found: C, 61.10; H, 4.26; N, 7.84.

RESULTS AND DISCUSSION

Monomer Synthesis

Scheme 1 depicts the route followed for synthesis of new bio-based aromatic diacylhydrazide monomers, namely, DVHzC-3 and DSHzC-3. The starting materials, namely, vanillic acid, syringic acid, and 1,3-dibromopropane are all bio-based.^{50,51} Vanillic acid and syringic acid were converted into respective methyl esters and were further reacted with 1,3-dibromopropane to afford corresponding α, ω -diesters. α, ω -Diesters were reacted with excess hydrazine hydrate to obtain aromatic diacylhydrazide monomers. The overall yields of diacyl hydrazide were in the range 65–73% and synthetic procedure is convenient and straight forward. The diacylhydrazides and intermediates involved in their preparation were characterized by FT-IR, ^1H NMR, ^{13}C NMR spectroscopy, HRMS, and elemental analyses.

FT-IR spectrum of DSHzC-3 is shown in Supporting Information Figure S1. FT-IR spectrum showed absorption bands at 3353 cm^{-1} and 1642 cm^{-1} corresponding to $-\text{NH}-/-\text{NH}_2$ and $-\text{C}=\text{O}$ group, respectively. A representative ^1H NMR spectrum of DSHzC-3 is reproduced in Figure 1.

The singlets appeared at $9.71\text{ }\delta$ ppm and $4.47\text{ }\delta$ ppm are attributed to $-\text{NH}-$ and $-\text{NH}_2$ protons, respectively. The aromatic protons exhibited a singlet at $7.15\text{ }\delta$ ppm. The methylene protons attached to oxygen atom showed a triplet

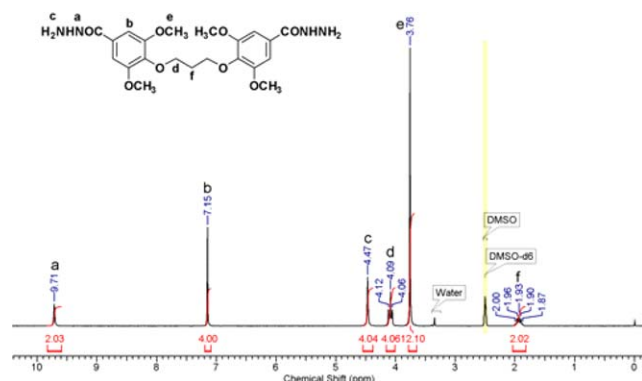


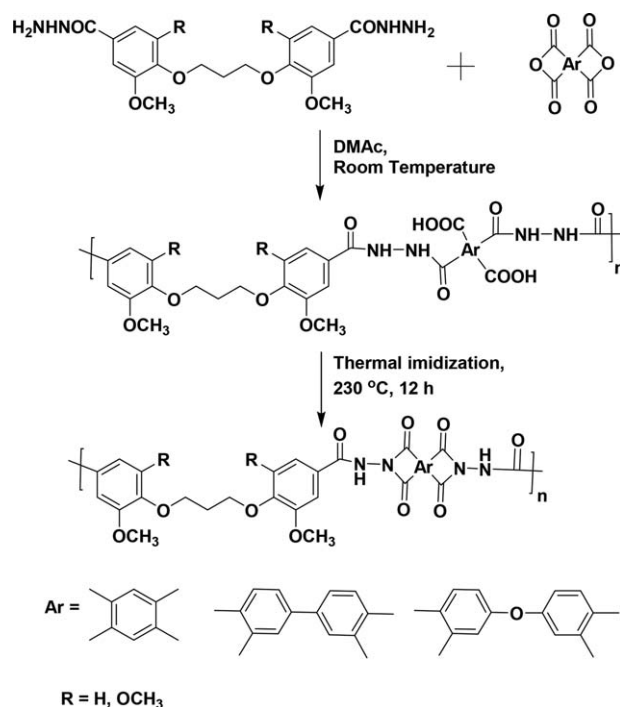
FIGURE 1 ^1H NMR Spectrum of 4,4'-(propane-1,3-diylbis(oxy))-bis(3,5-dimethoxybenzohydrazide) in $\text{DMSO}-d_6$. [Color figure can be viewed at wileyonlinelibrary.com]

at $4.09\text{ }\delta$ ppm and methoxy protons attached to aromatic ring appeared as a singlet at $3.76\text{ }\delta$ ppm. The remaining methylene protons showed a multiplet in the range $1.87\text{--}2.0\text{ }\delta$ ppm. ^{13}C NMR and HRMS spectral data of diacylhydrazides were in good agreement with the proposed structures.

Synthesis of Poly(amide imide)s

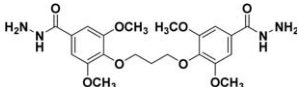
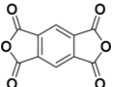
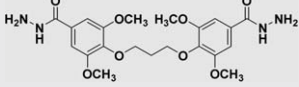
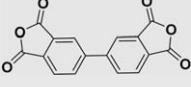
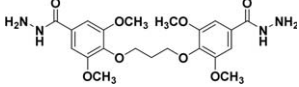
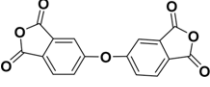
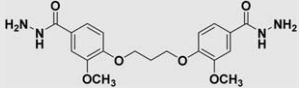
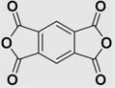
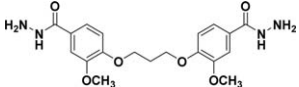
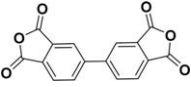
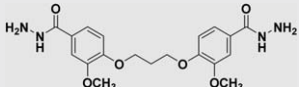
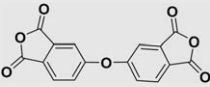
A series of new partially bio-based poly(amide imide)s was synthesized by polycondensation of diacylhydrazide monomers, namely, DVHzC-3 and DSHzC-3 with commercially available aromatic dianhydrides, namely, PMDA, BPDA, and OPA by two-step polycondensation reaction (Scheme 2). In the first step, poly(hydrazide acid) was synthesized by addition of stoichiometric quantity of aromatic dianhydride to the solution of diacylhydrazide in DMAc at room temperature.

The polycondensation reactions proceeded in a homogenous solution throughout the course of reaction. In the second step, cyclization of poly(hydrazide acid) was carried out by thermal cyclo-imidization method. The poly(hydrazide acid) solution was poured into a glass petri dish and solvent was evaporated by heating at $80\text{ }^\circ\text{C}$ with continuous nitrogen flow. The semi-dried poly(hydrazide acid) film was heated at



SCHEME 2 Synthesis of partially bio-based aromatic poly(amide imide)s.

TABLE 1 Inherent Viscosity, Molecular Weight and Thermomechanical Properties of Poly(amide imide)

Poly(amide imide)	Diacylhydrazide	Dianhydride	η_{inh} (dL g ⁻¹) ^a	GPC ^b		Dispersity	T_{10}^c (°C)	T_g^d (°C)	T_g^e (°C)	E' (Pa) $\times 10^9$ ^f
				$\bar{M}_n \times 10^3$	$\bar{M}_w \times 10^3$					
PAI-1			0.53	38.4	67.8	1.7	355	ND	248	3.5
PAI-2			0.56	40.8	72.6	1.7	356	223	246	2.2
PAI-3			0.47	36.6	63.0	1.7	352	209	238	3.0
PAI-4			0.44	25.5	53.5	2.0	340	218	226	1.6
PAI-5			0.51	37.0	66.6	1.8	360	212	224	0.4
PAI-6			0.45	29.4	56.0	1.9	364	201	214	1.1

^a η_{inh} was measured with 0.5% (w/v) solution of poly(amide imide) in DMAc at 30 ± 0.1 °C.

^b Measured by GPC in DMF, polystyrenes were used as the calibration standard.

^c Temperature at which 10% weight loss was observed.

^d T_g determined by DSC.

^e T_g determined by DMA.

^f Storage modulus measured at 50 °C. ND Not detected.

230 °C under reduced pressure for 12 h to form poly(amide imide).⁴⁵

The results of polymerization reactions are summarized in Table 1. Inherent viscosity values of poly(amide imide)s were in the range 0.44–0.56 dL g⁻¹. Poly(amide imide)s were soluble in DMF and their molecular weights were measured by GPC using polystyrenes as calibration standards. Number average molecular weights (\bar{M}_n) and dispersity values were in the range 25,500–40,800 and 1.7–2.0, respectively. Inherent viscosity values and GPC molecular weight data indicated the formation of reasonably high molecular weight polymers. Poly(amide imide)s being semi-rigid in nature, the \bar{M}_n values reported with polystyrene standards are expected to be overestimated. Similar observations have been reported in the literature for measurements of molecular weight by GPC of polymers which adopt a rod-like conformation in solution.^{52,53} Poly(amide imide)s could be cast into transparent, flexible, and tough film from their DMAc solution.

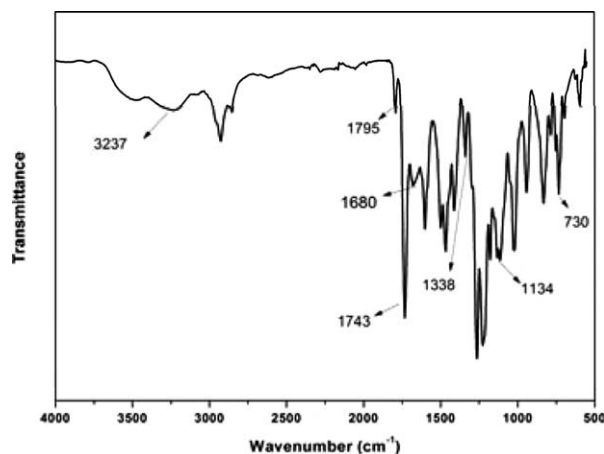
Structural Characterization of Poly(amide imide)s

The chemical structures of poly(amide imide)s were confirmed by FT-IR, ¹H and ¹³C NMR spectroscopy, and elemental analyses.

FT-IR spectrum of PAI-1 is reproduced in Figure 2. The absorption band at 3237 cm⁻¹ corresponds to —NH— of amide

linkage. The absorption band of the five membered imide carbonyl appeared at 1795 cm⁻¹ and 1743 cm⁻¹ corresponding to asymmetric and symmetric stretching vibration, respectively. A band at 1680 cm⁻¹ appeared due to carbonyl group of amide. The absorption bands at 1338 cm⁻¹ and 730 cm⁻¹ were assigned to stretching and bending vibrations, respectively, of C—N—C linkage of imide ring.⁴⁵

¹H NMR spectrum of PAI-1 is reproduced in Figure 3. A multiplet in the range 1.99–2.04 δ ppm was observed due to

**FIGURE 2** FT-IR spectrum of PAI-1.

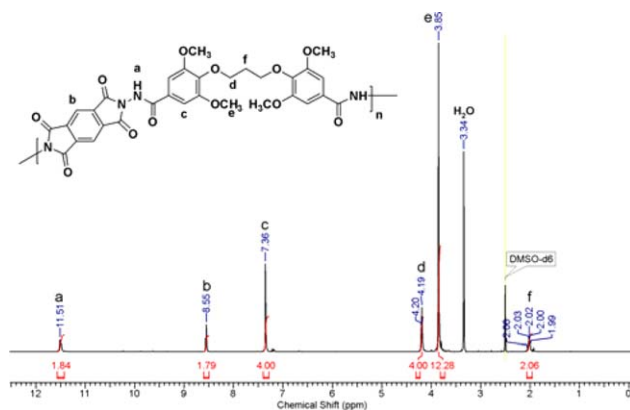


FIGURE 3 ^1H NMR spectrum of PAI-1 in $\text{DMSO}-d_6$. [Color figure can be viewed at [wileyonlinelibrary.com](#)]

methylene protons β to oxygen atom. Methoxy protons exhibited a singlet at 3.85δ ppm while methylene protons attached to oxygen atom appeared as a triplet at 4.19δ ppm. Aromatic protons *ortho* to amide group displayed a singlet at 7.36δ ppm. The aromatic protons of PMDA moiety appeared as a singlet at 8.55δ ppm. Amide protons ($-\text{NH}-$) exhibited a broad singlet at 11.51δ ppm. ^{13}C NMR spectrum of PAI-1 along with assignments of carbon atoms is reproduced in Supporting Information Figure S2.

Solubility of Poly(amide imide)s

The solubility of poly(amide imide)s was investigated at 3% (w/v) in various organic solvents. Poly(amide imide)s exhibited good solubility in organic solvents such as DMF, DMAc, DMSO, NMP, pyridine, and m-cresol and were insoluble in chloroform and dichloromethane. The improvement in solubility characteristic of poly(amide imide)s could be attributed to the combined effect of flexible oxypropylene linkages and polar methoxy substituents.

X-ray Diffraction Studies of Poly(amide imide)s

X-ray diffractograms of poly(amide imide)s are shown in Figure 4. Poly(amide imide)s exhibited two broad halos in the range $2\theta = 20\text{--}30^\circ$ and $10\text{--}15^\circ$. The broad halos in XRD patterns indicated their amorphous nature, which could be mainly because of the presence of methoxy substituents which disrupt close packing of polymer chains.

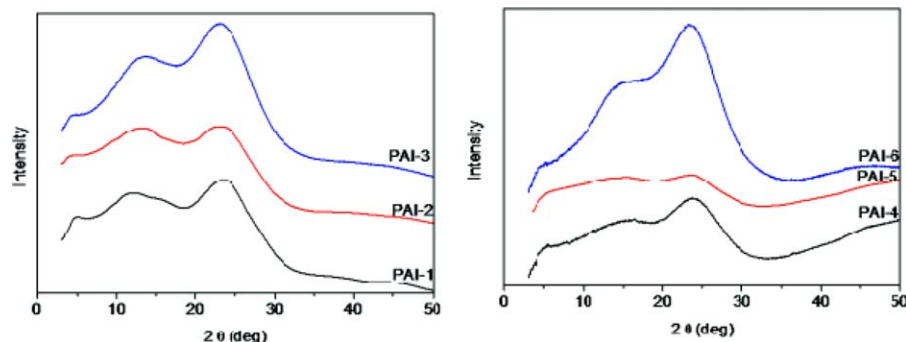


FIGURE 4 X-Ray diffractograms of poly(amide imide)s. [Color figure can be viewed at [wileyonlinelibrary.com](#)]

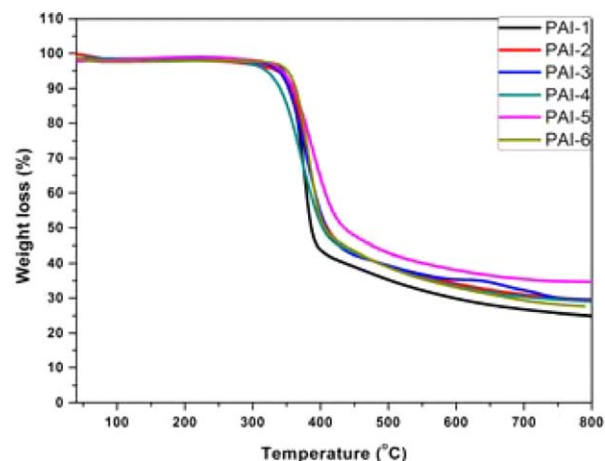


FIGURE 5 TG curves of poly(amide imide)s. [Color figure can be viewed at [wileyonlinelibrary.com](#)]

Thermal Properties of Poly(amide imide)s

The thermal properties of poly(amide imide)s were evaluated by TGA and DSC at a heating rate of $10^\circ\text{C min}^{-1}$ under nitrogen atmosphere. TG and DSC curves are shown in Figures 5 and 6, respectively, and the data are summarized in Table 1. The 10% weight loss temperatures of poly(amide imide)s under nitrogen atmosphere were in the range $340\text{--}364^\circ\text{C}$, indicating their acceptable thermal stability. However, the thermal stability (T_{10} values) of present poly(amide imide)s are inferior compared with the conventional fully aromatic poly(amide imide)s^{42,44}. The lowering of thermal stability could be attributed to the presence of thermally labile oxypropylene linkages and methoxy groups. The weight residues of poly(amide imide)s at 800°C were in the range $24\text{--}34\%$, which could be attributed to the formation of carbonaceous materials due to anaerobic heating of the polymers. T_g values of poly(amide imide)s were in the range $201\text{--}223^\circ\text{C}$ except for PAI-1 which did not show T_g in DSC analysis.

DMA of Poly(amide imide)s

The thermomechanical properties of poly(amide imide)s were determined by DMA. DMA curves of poly(amide imide)s are displayed in Figure 7 and the data are included in Table 1. The storage modulus of oxypropylene containing

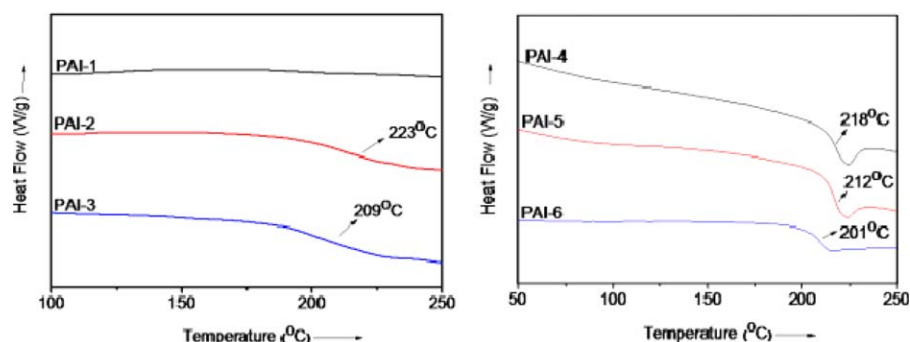


FIGURE 6 DSC curves of poly(amide imide)s. [Color figure can be viewed at wileyonlinelibrary.com]

poly(amide imide)s based on DSHzC-3 and DVHzC-3 were in the range 2.2×10^9 to 3.5×10^9 and 0.4×10^9 to 1.6×10^9 Pa, respectively, indicating their high mechanical strength. Results showed that poly(amide imide)s based on DSHzC-3 exhibited higher storage modulus than corresponding poly(amide imide)s based on DVHzC-3 which could be attributed to the higher chain rigidity imposed by additional methoxy substituents.

All the poly(amide imide)s showed two transitions above room temperature. The transition appearing at higher temperature, that is, the α transition, corresponds to T_g . The transition that appeared in the temperature range 122–155 °C corresponds to the sub-glass transition or β transition.⁵⁴ The T_g values of poly(amide imide)s were in the range 214–248 °C and these values were slightly higher compared with corresponding T_g values measured by DSC. The difference in T_g values by DMA and DSC may be due to different principles of measurements; DMA measures the mechanical response while DSC records the changes in heat flow of polymer.

It was noticed that T_g values of poly(amide imide)s based on both diacylhydrazides followed the order: ODPDA < BPDA < PMDA. The lowest T_g observed for ODPDA-based poly(amide imide)s could be explained on the basis of introduction of additional ether linkages while the highest T_g values of PMDA-based poly(amide imide)s are attributed to rigidity imparted by the rigid dianhydride monomer. The

similar trends in T_g values have been reported in the literature for polyimides and poly(amide imide)s.⁴⁸

The effects of methoxy substituents in diacylhydrazide monomers on T_g values of corresponding poly(amide imide)s were evaluated. Poly(amide imide)s derived from tetramethoxy substituted diacylhydrazide, namely, DSHzC-3, showed higher T_g values than corresponding poly(amide imide)s based on dimethoxy substituted diacylhydrazide, namely, DVHzC-3. MD simulation studies were performed on selected poly(amide imide)s to analyze the molecular origin of the observed substituent effects on T_g .

MD Simulation Studies of Representative Poly(amide imide)s (PAI-1 and PAI-4)

Two representative poly(amide imide)s, namely, PAI-1 and PAI-4, which differ in the number of methoxy substituents on aromatic rings were selected for MD simulation studies. All atomistic models of the repeating units of poly(amide imide)s are shown in Supporting Information Figure S5. The details of polymer melt preparation, equilibration, and simulation procedure are given in Supporting Information. The simulation studies were carried out using Gromacs-5.0.5⁵⁵ package and OPLA-AA⁵⁶ force field (see Supporting Information for simulation details). T_g values of PAI-1 and PAI-4 were calculated from temperature dependence of the density as shown in Figure 8. This approach of T_g calculation has been used previously for polyimides by Lyulin et al.⁵⁷ The calculated T_g values were higher compared with the

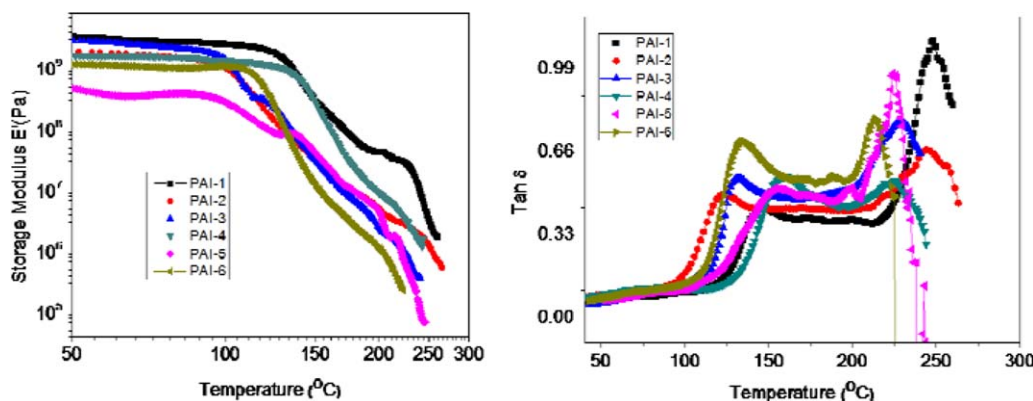


FIGURE 7 Dynamic mechanical curves of poly(amide imide)s. [Color figure can be viewed at wileyonlinelibrary.com]

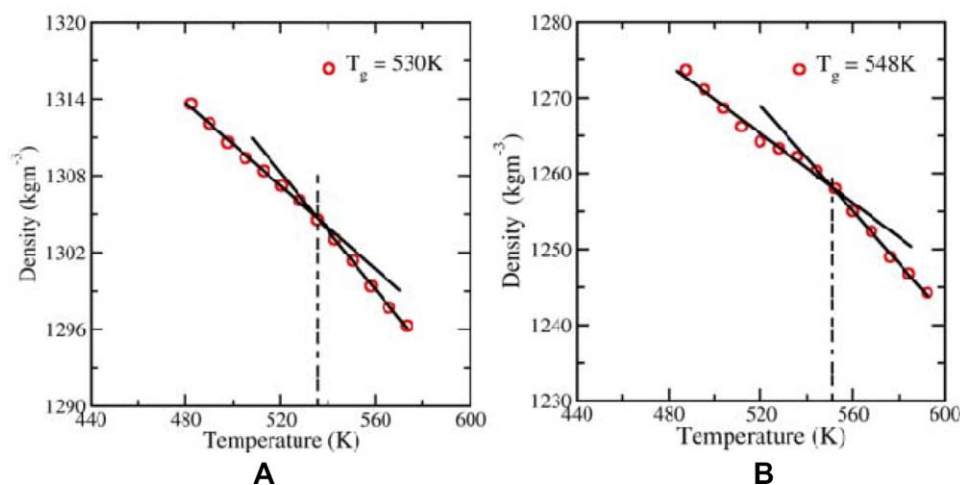


FIGURE 8 T_g of poly(amide imide)s measured by MD simulation. (A) Poly(amide imide) based on DVHzC-3 (PAI-4). (B) Poly(amide imide) based on DSHzC-3 (PAI-1). [Color figure can be viewed at wileyonlinelibrary.com]

corresponding experimental values obtained from DMA studies due to the higher cooling rates applied (10 K ns^{-1}) in simulation studies. However, the shift in the experimental T_g value has been well reproduced. The calculated T_g of PAI-1 is 18 K higher than PAI-4 as compared with an increase in 22 K observed in DMA studies. It is generally accepted that T_g of an amorphous polymer is determined by α relaxation or segmental motion of the chains,⁵⁸ which in turn is affected by the free volume⁵⁹ and/or rigidity⁶⁰ of the chains. The availability of more free volume and less chain rigidity leads to faster relaxation resulting in lower T_g and vice versa. However, prior studies indicate that these two factors might work independently and either of them can be a controlling factor in affecting T_g .^{61,62} The calculated free volume, densities along with other physical properties of PAI-1 and PAI-4 are shown in Supporting Information Table S1. Interestingly, despite having higher T_g , PAI-1 showed lower density and higher free volume as compared with PAI-4. The density of PAI-1 and PAI-4 would depend on the intra- as well as inter-chain spacing/packing. The higher radius of gyration (Supporting Information Table S1) of PAI-1 indicated a slightly expanded conformation that leads to the

lower density. The radial distribution function (RDF) between the centers of mass of all the chains [Supporting Information Figure S7(A)] showed the first peak at a larger distance for PAI-1 depicting higher inter-chain spacing. Similarly, RDF between the centers of mass of the phenyl rings and all other atoms within single chains also showed peak at a larger distance for PAI-1 [Supporting Information Figure S7(B)]. This points out that the chains expand and span larger volume in the case of PAI-1. Thus, more inter- and intra- chain spacing in PAI-1 leads to higher free volume and lesser density. Representative snapshots showing inter-chain spacing for PAI-1 and PAI-4 are shown in Supporting Information Figure S8. Similar counterintuitive observations of increased T_g accompanied with decreased density have been reported by Nair and coworkers⁶³ for polyimide-HFPE-30 and Gu and coworkers⁶⁴ for polyimide based on BPDA and 4,4'-oxydianiline. In both the studies, density of the higher T_g polymer was reported to be lesser than its counterpart. These reports attributed the observed increase in T_g with substitution and isomerization to the increased rigidity of polymer backbone. Both these studies have demonstrated higher rotational barrier associated with groups involving substitution or isomerization.

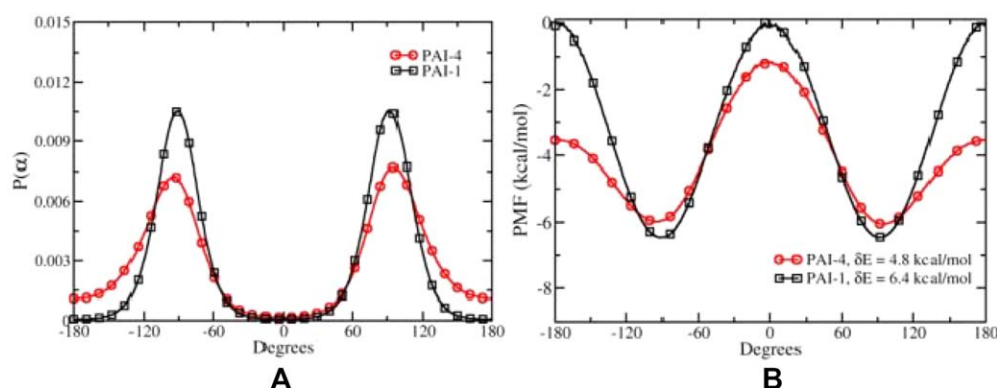


FIGURE 9 (A) Torsional angle distributions of PAI-4 and PAI-1. (B) Rotational energy barrier from PMF for PAI-4 and PAI-1. [Color figure can be viewed at wileyonlinelibrary.com]

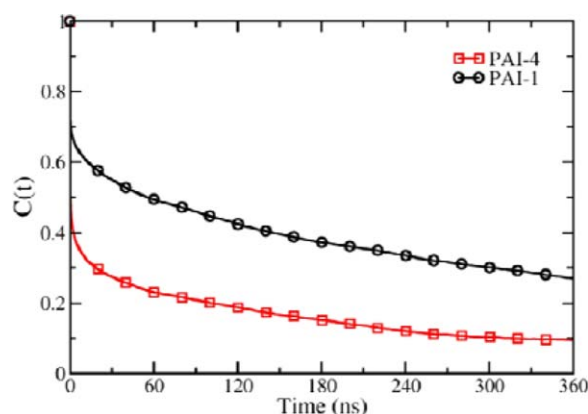


FIGURE 10 Comparison of the decay of dihedral autocorrelation function ($C(t)$) for PAI-4 and PAI-1. [Color figure can be viewed at wileyonlinelibrary.com]

Along the similar lines, effect of the chain rigidity, in particular the rotational barrier between the phenyl ring and the oxypropylene linkage on respective T_g values was explored. Torsional angle distribution of α [see Supporting Information Figure S5(A) for a structural representation] is shown in Figure 9(A). The dramatic increase in the peak intensities in PAI-1 indicated that the rotation around phenyl ring is more hindered due to the extra methoxy substituents. To quantify the increase in the rotational barrier with substitution, potential of mean force (PMF), $G(\alpha)$ was calculated from the torsional distributions using the Boltzmann inversion relation:

$$G(\alpha) = -k_B T \ln P(\alpha)$$

The difference between the minima and maxima of PMF [Figure 9(B)] corresponds to the free energy barrier for torsional rotation. PAI-1 exhibited $1.6 \text{ kcal mol}^{-1}$ higher rotational barrier than PAI-4. Thus, in PAI-1 rotation around phenyl ring is hindered, which restricts the segmental motion and thereby increases the relaxation time. To analyze the segmental relaxation, dihedral autocorrelation function⁶³ $C(t)$ was calculated as follows:

$$C(t) = \langle \cos [\alpha(t) - \alpha(t + \Delta t)] \rangle_t$$

where $\alpha(t)$ and $\alpha(t + \Delta t)$ denote the torsional angle at time t and time $t + \Delta t$, respectively. The time-scale of decay of $C(t)$ gives a measure of the rigidity of chains, where a longer time-scale would signify increased rigidity.⁶⁰ The comparison of $C(t)$ for both PAI-4 and PAI-1 is shown in Figure 10. It was observed that the decay in $C(t)$ for PAI-1 is substantially slower than PAI-4 indicating the higher rigidity due to hindered backbone rotation. Thus, the MD simulation data clearly established that molecular origin of the increased T_g in PAI-1 as compared with PAI-4 is the increase in the rotational barrier between the substituted aromatic rings. This leads to substantially slower segmental relaxation and increased rigidity in the polymer chain.

CONCLUSIONS

Two new bio-based diacylhydrazide monomers were synthesized starting from vanillic acid, syringic acid, and 1,3-

dibromopropane. A series of new partially bio-based poly(amide imide)s was prepared from diacylhydrazides and commercially available aromatic dianhydrides. Poly(amide imide)s exhibited amorphous nature and good solubility in polar solvents. Poly(amide imide)s could be cast into transparent, flexible, and tough films from their DMAc solutions. Poly(amide imide)s showed inherent viscosity and M_n in the range $0.44\text{--}0.56 \text{ dL g}^{-1}$ and $25,500\text{--}40,800$, respectively. Poly(amide imide)s showed 10% weight loss in the temperature range $340\text{--}364^\circ\text{C}$ indicating their acceptable thermal stability. Thermomechanical properties of poly(amide imide)s were studied by DMA which indicated that poly(amide imide)s based on DSHzC-3 exhibited higher storage modulus than corresponding poly(amide imide)s based on DVHzC-3. Both DMA and DSC showed higher T_g for poly(amide imide)s based on DSHzC-3 compared with the corresponding poly(amide imide)s based on DVHzC-3. MD simulation studies on representative poly(amide imide)s indicated that chain rigidity, imposed by additional methoxy substituents on phenyl ring, as the molecular origin for the observed increase in T_g of poly(amide imide)s based on DSHzC-3. As a final remark, vanillic acid, and syringic acid represent valuable precursors for the synthesis of difunctional monomers useful in the preparation of high performance/temperature thermoplastic polymers.

ACKNOWLEDGMENTS

The authors thank CSIR-4PI supercomputing facility for the computational resources. This work was supported by a fellowship from the University Grants Commission (UGC), New Delhi, India (to S.S.K.), Senior Research Fellowship from CSIR, New Delhi (to P.S.), and the Ramanujan Fellowship from the Department of Science and Technology (DST), India (SR/S2/RJN-84/2012) (to S.C.).

REFERENCES AND NOTES

- 1 R. Mülhaupt, *Macromol. Chem. Phys.* **2013**, *214*, 159.
- 2 A. Gandini, T. M. Lacerda, A. J. F. Carvalho, E. trovatti, *Chem. Rev.* **2016**, *116*, 1637.
- 3 A. Gandini, *Macromolecules*. **2008**, *41*, 9491.
- 4 F. Fenouillot, A. Rousseau, G. Colomines, R. Saint-Loup, J. P. Pascault, *Prog. Polym. Sci.* **2010**, *35*, 578.
- 5 P. R. Wool, X. S. Sun, *Bio-Based Polymers and Composites*; Elsevier: Amsterdam, **2005**; pp. 1–640.
- 6 D. Dakshinamoorthy, S. P. Lewis, M. P. Cavazza, A. M. Hoover, D. F. Iwig, K. Damodaran, R. T. Mathers, *Green Chem.* **2014**, *16*, 1774.
- 7 D. K. Schneiderman, M. A. Hillmyer, *Macromolecules* **2017**, *50*, 3733.
- 8 M. Bocqué, C. Voirin, V. Lapinte, S. Caillol, J. J. Robin, *J. Polym. Sci. Part A: Polym. Chem.* **2016**, *54*, 11.
- 9 G. Lligadas, J. C. Ronda, M. Galià, V. J. Cádiz, *Polym. Sci. Part A: Polym. Chem.* **2013**, *51*, 2111.
- 10 L. Montero, D. Espinosa, M. A. R. Meier, *Eur. Polym. J.* **2011**, *47*, 837.
- 11 F. Seniha Güner, Y. Yağcı, A. Tuncer Erciyes, *Prog. Polym. Sci.* **2006**, *31*, 633.

- 12 D. J. Liaw, K. L. Wang, Y. C. Huang, K. R. Lee, J. Y. Lai, C. S. Ha, *Prog. Polym. Sci.* **2012**, *37*, 907.
- 13 J. M. García, F. C. García, F. Serna, J. L. de la Peña, *Prog. Polym. Sci.* **2010**, *35*, 623.
- 14 A. Llevot, E. Grau, S. Carlotti, S. Grelrier, H. Cramail, *Macromol. Rapid Commun.* **2016**, *37*, 9.
- 15 M. Fache, B. Boutevin, S. Caillol, *Eur. Polym. J.* **2015**, *68*, 488.
- 16 F. H. Isikgor, C. R. Becer, *Polym. Chem.* **2015**, *6*, 4497.
- 17 A. Gandini, D. Coelho, M. Gomes, B. Reis, A. J. Silvestre, *Mater. Chem.* **2009**, *19*, 8656.
- 18 C. Voirin, S. Caillol, N. V. Sadavarte, B. V. Tawade, B. Boutevin, P. P. Wadgaonkar, *Polym. Chem.* **2014**, *5*, 3142.
- 19 D. Chatterjee, N. V. Sadavarte, R. D. Shingate, A. S. More, B. V. Tawade, A. D. Kulkarni, A. B. Ichake, C. V. Avadhani, P. P. Wadgaonkar, In *Cashew Nut Shell Liquid A Goldfield for Functional Materials*, P. Anilkumar, Ed., 1st ed.; Springer: Switzerland, **2017**; Chapter 9, pp. 163–214.
- 20 B. G. Harvey, A. J. Guenther, T. A. Koontz, P. J. Storch, J. T. Reams, T. J. Groshens, *Green Chem.* **2016**, *18*, 2416.
- 21 J. Qin, H. Liu, P. Zhang, M. Wolcott, J. Zhang, *Polym. Int.* **2014**, *63*, 760.
- 22 A. Kumar, S. Tateyama, K. Yasaki, M. A. Ali, N. Takaya, R. Singh, T. Kaneko, *Polymer* **2016**, *83*, 182.
- 23 D. Watkins, M. Nuruddin, M. Hosur, A. Tcherbi-Narteh, S. Jeelani, *J. Mater. Res. Technol.* **2015**, *4*, 26.
- 24 S. Laurichesse, L. Avérous, *Prog. Polym. Sci.* **2014**, *39*, 1266.
- 25 M. Fache, E. Darroman, V. Besse, R. Auvergne, S. Caillol, B. Boutevin, *Green Chem.* **2014**, *16*, 1987.
- 26 J. F. Stanzione, J. M. Sadler, J. J. La Scala, K. H. Reno, R. P. Wool, *Green Chem.* **2012**, *14*, 2346.
- 27 M. Fache, R. Auvergne, B. Boutevin, S. Caillol, *Eur. Polym. J.* **2015**, *67*, 527.
- 28 N. K. Sini, J. Bijwe, I. K. Varma, *J. Polym. Sci. Part A: Polym. Chem.* **2014**, *52*, 7.
- 29 H. A. Meylemans, B. G. Harvey, J. T. Reams, A. J. Guenther, L. R. Cambrea, T. J. Groshens, L. C. Baldwin, M. D. Garrison, J. M. Mabry, *Biomacromolecules* **2013**, *14*, 771.
- 30 B. G. Harvey, A. J. Guenther, H. A. Meylemans, S. R. L. Haines, K. R. Lamison, T. J. Groshens, L. R. Cambrea, M. C. Davis, W. W. Lai, *Green Chem.* **2015**, *17*, 1249.
- 31 F. Pion, P. H. Ducrot, F. Allais, *Macromol. Chem. Phys.* **2014**, *215*, 431.
- 32 L. Mialon, R. Vanderhenst, A. G. Pemba, S. A. Miller, *Macromol. Rapid Commun.* **2011**, *32*, 1386.
- 33 S. S. Kuhire, S. S. Nagane, P. P. Wadgaonkar, WO2015140818A1.
- 34 L. Mialon, A. G. Pemba, S. A. Miller, *Green Chem.* **2010**, *12*, 1704.
- 35 C. Pang, J. Zhang, Q. Zhang, G. Wu, Y. Wang, J. Ma, *Polym. Chem.* **2015**, *6*, 797.
- 36 A. G. Pemba, M. Rostagno, T. A. Lee, S. A. Miller, *Polym. Chem.* **2014**, *5*, 3214.
- 37 S. S. Kuhire, C. V. Avadhani, P. P. Wadgaonkar, *Eur. Polym. J.* **2015**, *71*, 547.
- 38 P. P. Wadgaonkar, S. S. Kuhire, WO2016103283A1.
- 39 M. Ding, *Prog. Polym. Sci.* **2007**, *32*, 623.
- 40 D. M. Stoakley, A. K. St. Clair, C. I. Croall, *J. Appl. Polym. Sci.* **1994**, *51*, 1479.
- 41 M. K. Ghosh, K. L. Mittal, *Polyimides: Fundamentals and Applications*; Marcel Dekker Inc: New York, **1996**; pp. 1–912.
- 42 M. J. Dodda, P. Bělský, *Eur. Polym. J.* **2016**, *84*, 514.
- 43 X. M. Zhang, J. G. Liu, S. Y. Yang, *Rev. Adv. Mater. Sci.* **2016**, *46*, 22.
- 44 W. Wrasidlo, J. J. Augl, *Polym. Sci. Part A: Polym. Chem.* **1969**, *7*, 321.
- 45 A. S. More, A. S. Patil, P. P. Wadgaonkar, *Polym. Degrad. Stab.* **2010**, *95*, 837.
- 46 C. V. Avadhani, P. P. Wadgaonkar, S. P. Vernekar, *J. Appl. Polym. Sci.* **1990**, *40*, 1325.
- 47 C. Yang, G. Liou, C. Yang, S. Chen, T. Hsiang, *Polym. Bull.* **1999**, *28*, 21.
- 48 V. S. Nilakshi, C. V. Avadhani, V. N. Parimal, P. P. Wadgaonkar, *Eur. Polym. J.* **2010**, *46*, 1307.
- 49 D. D. Perrien, W. L. F. Armerego, *Purification of Laboratory Chemicals*, 3rd ed.; Pergamon Press: Oxford, **1988**, pp. 1–392.
- 50 B. Lochab, S. Shukla, I. K. Varma, *RSC Adv.* **2014**, *4*, 21712.
- 51 Y. S. Jang, B. Kim, J. H. Shin, Y. J. Choi, S. Choi, C. W. Song, J. Lee, H. G. Park, S. Y. Lee, *Biotechnol. Bioeng.* **2012**, *109*, 2437.
- 52 J. Liu, R. S. Loewe, R. D. McCullough, *Macromolecules* **1999**, *32*, 5777.
- 53 J. M. Lupton, K. Becker, G. Gaefke, J. Rolffs, S. Ho, *Chem. Commun.* **2010**, *46*, 4686.
- 54 F. E. Arnold, K. R. Bruno, D. Shen, M. Eashoo, C. J. Lee, F. W. Harris, S. Z. D. Cheng, *Polym. Eng. Sci.* **1993**, *33*, 1373.
- 55 B. Hess, C. Kutzner, D. E. van der Spoel, Lindahl, *J. Chem. Theory Comput.* **2008**, *4*, 435.
- 56 W. L. Jorgensen, D. S. Maxwell, J. Tirado-Rives, *J. Am. Chem. Soc.* **1996**, *118*, 11225.
- 57 S. V. Lyulin, S. V. Larin, A. A. Gurtovenko, V. M. Nazarychev, S. G. Falkovich, V. E. Yudin, V. M. Svetlichnyi, I. V. Gofman, A. V. Lyulin, *Soft Matter* **2014**, *10*, 1224.
- 58 A. Arbe, F. Alvarez, J. Colmenero, *Soft Matter* **2012**, *8*, 8257.
- 59 R. P. White, J. E. G. Lipson, *Macromolecules* **2016**, *49*, 3987.
- 60 X. Li, A. F. Yee, *Macromolecules* **2003**, *36*, 9411.
- 61 V. P. Privalko, Y. S. Lipatov, *Macromol. Sci. Part B: Phys.* **1974**, *9*, 551.
- 62 T. T. Hsieh, C. Tiu, G. P. Simon, *J. Appl. Polym. Sci.* **2001**, *82*, 2252.
- 63 S. Pandiyan, P. V. Parandekar, O. Prakash, T. K. Tsotsis, N. N. Nair, S. Basu, *Chem. Phys. Lett.* **2014**, *593*, 24.
- 64 M. Li, X. Y. Liu, J. Q. Qin, Y. Gu, *Express Polym. Lett.* **2009**, *3*, 665.